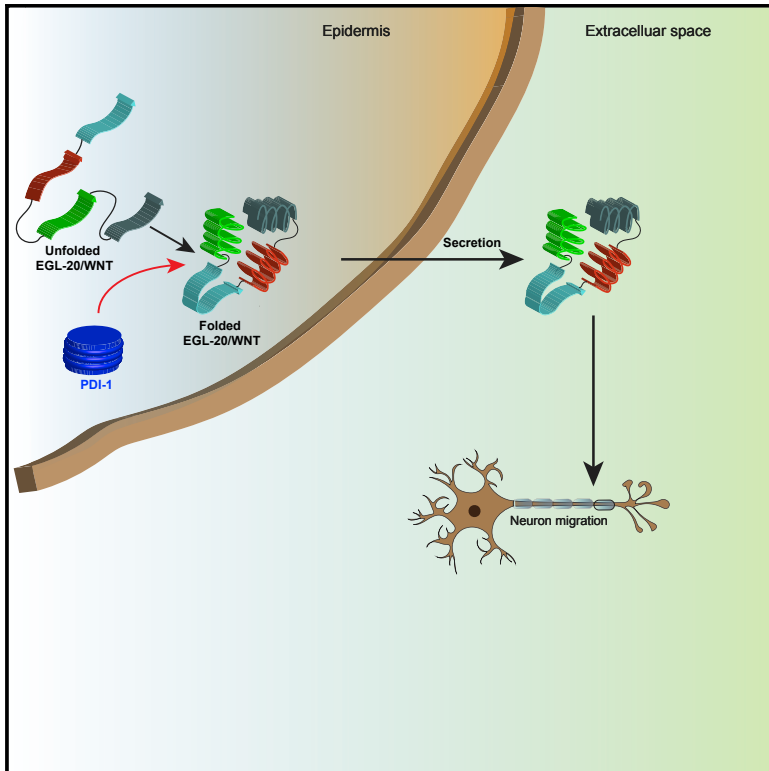


Cell Reports

A Protein Disulfide Isomerase Controls Neuronal Migration through Regulation of Wnt Secretion

Graphical Abstract



Authors

Nanna Torpe, Sandeep Gopal, Oguzhan Baltaci, Lorenzo Rella, Ava Handley, Hendrik C. Korswagen, Roger Pocock

Correspondence

roger.pocock@monash.edu

In Brief

Wnt proteins are conserved regulators of developmental patterning. Here, Torpe et al. report that Wnt secretion is regulated by a protein disulfide isomerase in *Caenorhabditis elegans* and human cells.

Highlights

- PDI-1, a protein disulfide isomerase, regulates neuron migration
- PDI-1 functions in EGL-20/Wnt-producing cells to control neuron migration
- Protein disulfide isomerases are evolutionarily conserved regulators of Wnt secretion



A Protein Disulfide Isomerase Controls Neuronal Migration through Regulation of Wnt Secretion

Nanna Torpe,^{2,4} Sandeep Gopal,^{1,4} Oguzhan Baltaci,¹ Lorenzo Rella,^{2,3} Ava Handley,¹ Hendrik C. Korswagen,³ and Roger Pocock^{1,2,5,*}

¹Development and Stem Cells Program, Monash Biomedicine Discovery Institute and Department of Anatomy and Developmental Biology, Monash University, Melbourne, VIC 3800, Australia

²Biotech Research and Innovation Centre, University of Copenhagen, Ole Maaløes Vej 5, Copenhagen, Denmark

³Hubrecht Institute, Royal Netherlands Academy of Arts and Sciences and University Medical Center Utrecht, Uppsalalaan 8, 3584 CT Utrecht, the Netherlands

⁴These authors contributed equally

⁵Lead Contact

*Correspondence: roger.pocock@monash.edu
<https://doi.org/10.1016/j.celrep.2019.02.072>

SUMMARY

Appropriate Wnt morphogen secretion is required to control animal development and homeostasis. Although correct Wnt globular structure is essential for secretion, proteins that directly mediate Wnt folding and maturation remain uncharacterized. Here, we report that protein disulfide isomerase-1 (PDI-1), a protein-folding catalyst and chaperone, controls secretion of the *Caenorhabditis elegans* Wnt ortholog EGL-20. We find that PDI-1 function is required to correctly form an anteroposterior EGL-20/Wnt gradient during embryonic development. Furthermore, PDI-1 performs this role in EGL-20/Wnt-producing epidermal cells to cell-non-autonomously control EGL-20/Wnt-dependent neuronal migration. Using pharmacological inhibition, we further show that PDI function is required in human cells for Wnt3a secretion, revealing a conserved role for disulfide isomerases. Together, these results demonstrate a critical role for PDIs within Wnt-producing cells to control long-range developmental events that are dependent on Wnt secretion.

INTRODUCTION

Wnt glycoproteins are predominant regulators of metazoan cell fate patterning and tissue assembly. During development, Wnt proteins can form long-range concentration gradients to provide positional and instructive information to surrounding cells (Cadiogan et al., 1998; Clevers, 2006). The scale and amplitude of Wnt protein gradients require tight regulation, as aberrant gradient formation is linked to developmental deficits and disease (Christodoulides et al., 2006; MacDonald et al., 2014; Person et al., 2010; Roifman et al., 2015). As such, there is great interest in understanding how Wnt proteins are synthesized, modified, secreted, and delivered to receiving cells.

Wnt proteins are characterized by 24 invariantly positioned cysteine residues that form intramolecular disulfide bonds to maintain functional Wnt globular secondary structure (Miller, 2002; Willert and Nusse, 2012). Wnt protein synthesis and maturation occur in the endoplasmic reticulum (ER) and Golgi apparatus, facilitated by numerous processing enzymes and molecular chaperones (Braakman and Bulleid, 2011; Willert and Nusse, 2012). During Wnt maturation, complex folding events and posttranslational modifications occur to support secretion and formation of a Wnt concentration gradient (Janda et al., 2012; Willert and Nusse, 2012). Biochemical characterization of secreted Wnt revealed that Wnt proteins undergo functionally important posttranslational modifications such as lipidation and glycosylation (Caramelo and Parodi, 2007; Takada et al., 2006; Willert et al., 2003). A particularly critical step for Wnt protein maturation and secretion is acylation of a specific serine residue by the membrane-bound O-acyltransferase called Porcupine (Kadowaki et al., 1996; van den Heuvel et al., 1993). Inhibiting Wnt protein acylation ablates Wnt signaling and causes developmental defects (Barrott et al., 2011; Grzeschik et al., 2007). Transfer of the acyl group to Wnt proteins is required for a functional interaction with Wntless (Wls), which binds to and conveys Wnt proteins to the cell surface—a critical process for correct Wnt secretion (Bänziger et al., 2006). Following delivery of Wnt protein, Wls is recycled to the Golgi via endosomes and the retromer complex where it may escort newly synthesized Wnt to the cell surface (Belenkaya et al., 2008; Coudreuse et al., 2006; Port et al., 2008; Prasad and Clark, 2006; Yang et al., 2008). In *Caenorhabditis elegans*, studies have shown that MIG-14/Wls and retromer complex components such as VPS-35 are required for appropriate formation of an EGL-20/Wnt gradient (Coudreuse et al., 2006; Yang et al., 2008). Furthermore, previous studies demonstrated that in the absence of retromer complex function, MIG-14/Wls is degraded in lysosomes, thereby limiting EGL-20/Wnt secretion (Yang et al., 2008). Therefore, key molecular components and mechanisms controlling Wnt secretion are highly conserved.

Wnt proteins play major roles in directing neuronal migration and axon-dendritic guidance in vertebrates (Bocchi et al.,



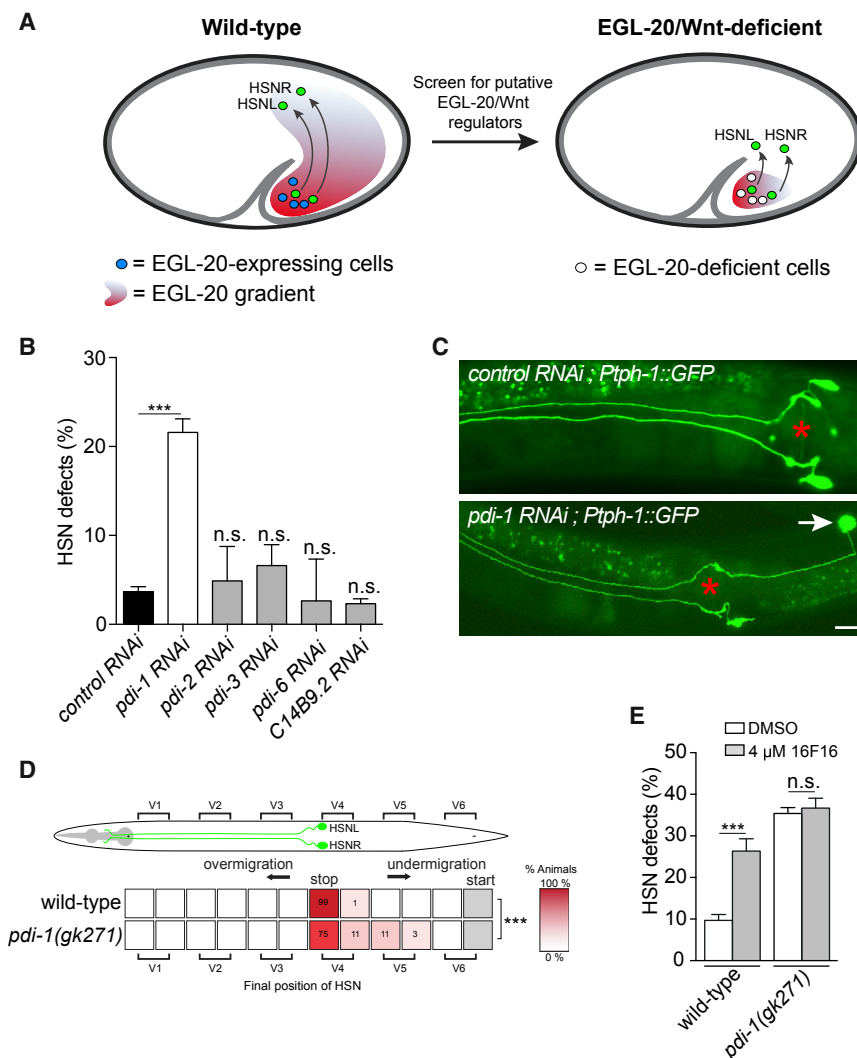


Figure 1. PDI-1 Controls HSN Migration

(A) EGL-20/Wnt forms a long-range morphogen gradient to control HSN migration during embryogenesis. This paradigm provides a screening platform to identify EGL-20/Wnt regulatory molecules.

(B) *pdi-1* RNAi knockdown causes HSN developmental defects. $n > 50$; *** $p < 0.001$; n.s., not significant (compared to vector control RNAi).

(C) HSN anatomy of young adults: control RNAi (upper image) and *pdi-1* RNAi (lower image). The *pdi-1* RNAi image shows the most common phenotype observed (undermigration, white arrow) when *pdi-1* expression is reduced (see Table S1 for details). Ventral view, anterior is to the left. Scale bar: 20 μ m.

(D) Average position of the HSNs with respect to seam cells V1.a to V6.p in wild-type and *pdi-1(gk271)* animals (scored by Nomarski optics). Values listed are percentiles of the total number of cells scored; the red coded heatmap displays the range of percentile values. $n > 30$; *** $p < 0.0001$.

(E) Quantification of HSN developmental defects after exposure of wild-type and *pdi-1(gk271)* animals to the 16F16 PDI inhibitor. $n > 50$; *** $p < 0.001$; n.s., not significant.

2017; Yoshikawa et al., 2003). In *C. elegans*, Wnt proteins also control specific neurodevelopmental events, including neuron migration, neuronal polarity, and axon guidance (Coudreuse et al., 2006; Hilliard and Bargmann, 2006; Pan et al., 2006). Furthermore, control of EGL-20/Wnt gradient formation by MIG-14/Wls and the retromer complex is required to control neuronal development (Coudreuse et al., 2006; Yang et al., 2008). We therefore exploited the correlation between Wnt gradient formation and neuronal development in *C. elegans* to identify regulators of Wnt secretion.

Wnt proteins are rich in disulfide bonds that are mostly formed during translation in the ER (Fass, 2012). Disulfide bonds enhance Wnt stability in the proteolytic and oxidizing extracellular environment to enable appropriate cell-to-cell communication. Coordination of disulfide bonds is a vital and pervasive step during Wnt biogenesis, as previous studies demonstrated that correct disulfide bond formation is required for Wnt secretion (MacDonald et al., 2014; Zhang et al., 2012). This suggests that regulatory enzymes that monitor and shuffle disulfide bonds

would be essential for appropriate Wnt secretion and signaling. Here, we identify protein disulfide isomerases (PDIs) as master controllers of Wnt secretion. Our genetic and pharmacological analysis of *C. elegans* PDI-1 reveal that it is required for EGL-20/Wnt gradient formation and controls EGL-20-directed neuron migration from EGL-20-producing epidermal cells. We further demonstrate that PDI function is conserved, as inhibition of PDI in human cells specifically impairs

RESULTS

PDI-1, a PDI, Regulates Neuronal Migration

EGL-20/Wnt is expressed and secreted from a subset of hypodermal (epidermal) and muscle cells in the posterior of *C. elegans* (Whangbo and Kenyon, 1999) (Figure 1A). EGL-20 function is critical for specific neurodevelopmental events, including anterior migration of the hermaphrodite-specific neurons (HSNs) (Desai et al., 1988) (Figure 1A). We used HSN development as a readout of EGL-20 function to identify molecules that control Wnt maturation and secretion (Figure 1). PDIs are a family of protein chaperones that reside in the ER to catalyze the formation (oxidation), breakage (reduction), and rearrangement (isomerization) of disulfide bonds (Wilkinson and Gilbert, 2004). Due to the importance of disulfide bond formation for Wnt secretion and function (MacDonald

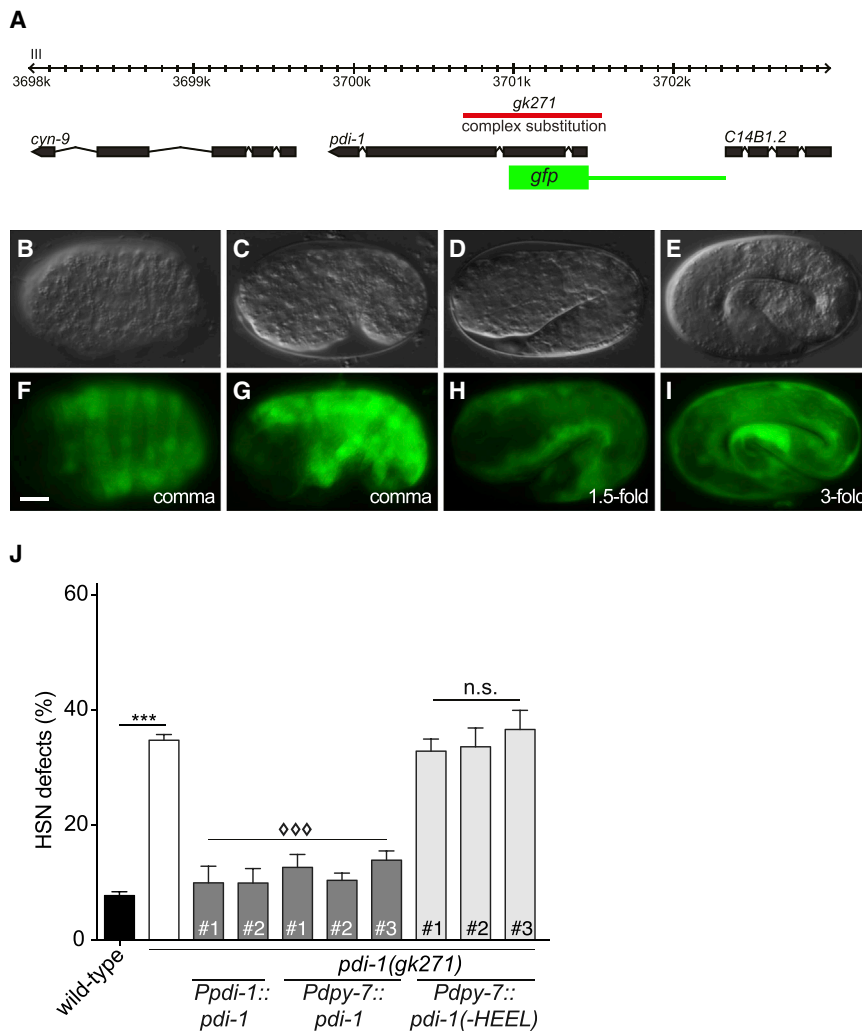


Figure 2. PDI-1 Regulates HSN Migration Cell-Non-Autonomously from the Epidermis

(A) Genetic locus of *pdi-1* showing gene structure in black and *gk271* genetic lesion in red. The 841-bp promoter used to drive *gfp* for expression analysis is in green.

(B–I) Expression of a *Ppdi-1::gfp* transcriptional reporter during embryonic development. Nomarski micrographs (B–E) and fluorescence images of the same embryos (F–I) are shown. Anterior is to the left. Scale bar: 10 μ m.

(J) HSN developmental defects of *pdi-1(gk271)* mutant animals are rescued by transgenic expression of *pdi-1* cDNA controlled by its own promoter and the hypodermal-specific *dpy-7* promoter. Deletion of the ER retention motif (–HEEL) abrogates PDI-1 rescuing ability in the hypodermis. n > 50; ***p = 0.001 for wild-type compared to *pdi-1(gk271)*; $\diamond \diamond \diamond$ p < 0.001; n.s., not significant for *pdi-1(gk271)* compared to rescue lines. # refers to independent transgenic lines. Scale bar: 10 μ m.

tion of QR.pax (Figure S2). Together, we show that PDI-1 controls two temporally distinct EGL-20-regulated migration events.

Using a previously reported PDI-specific 16F16 inhibitor, we asked whether manipulation of PDI activity could affect PDI-regulated HSN development *in vivo* (Hoffstrom et al., 2010; Kaplan et al., 2015). We found that 16F16 causes HSN defects in wild-type animals similar to that caused by loss of *pdi-1* (Figure 1E). In contrast, when *pdi-1(–)* animals were exposed to the PDI inhibitor, the HSN phenotype was not enhanced (Figure 1E),

suggesting that 16F16 causes HSN developmental defects by inhibiting of PDI-1 activity *in vivo*.

PDI-1 Regulates HSN Migration from Epidermal Cells

HSN migration occurs between the comma and 1.5-fold stages of embryogenesis (Desai et al., 1988). Using a GFP transgenic reporter for *pdi-1*, we detected GFP in embryonic hypodermis from the comma stage (Figures 2A–2I). We did not detect neuronal expression, suggesting that *pdi-1* regulates HSN development cell-non-autonomously, as shown for other guidance pathways (Kennedy et al., 2013; Pedersen et al., 2013).

To investigate the PDI-1 focus of action, we first drove *pdi-1* cDNA under the endogenous *pdi-1* promoter in *pdi-1(–)* animals and found that this fully rescued the *pdi-1(–)* HSN developmental defects (Figure 2J). We found that driving *pdi-1* cDNA under the hypodermal-specific *dpy-7* promoter also fully rescued the HSN defects of *pdi-1(–)* animals (Figure 2J). PDI proteins act in the ER lumen to catalyze protein folding and inhibit misfolded protein aggregation (Wilkinson and Gilbert, 2004). PDI

et al., 2014; Zhang et al., 2012), we hypothesized that PDIs may be important for EGL-20-directed HSN development. Using RNAi, we knocked down the expression of the five *C. elegans* PDI-encoding genes (*pdi-1*, *pdi-2*, *pdi-3*, *pdi-6*, and *C14B9.2*) and analyzed HSN development (Figures 1B and 1C). This screen identified a specific requirement for *pdi-1* during HSN development, where ~20% of *pdi-1(RNAi)*-treated animals exhibit an HSN undermigration phenotype (Figures 1B and 1C). We confirmed the role of *pdi-1* in HSN development using a previously isolated *pdi-1(gk271)*-null allele (Figures 1D, 1E, 2A, and S1; Table S1). As PDI proteins act as folding catalysts and molecular chaperones, we hypothesized that elevated temperature would exacerbate improper folding events and adversely affect HSN development. We indeed found that, in *pdi-1(–)* animals, HSN defects progressively increase with elevated incubation temperature (Figure S1). EGL-20 controls HSN migration during embryogenesis. To determine whether PDI-1 can also control EGL-20-dependent postembryonic neuronal development, we examined the post-embryonically migrating QR.pax cell. We found that *pdi-1(–)* animals also exhibit defective migra-

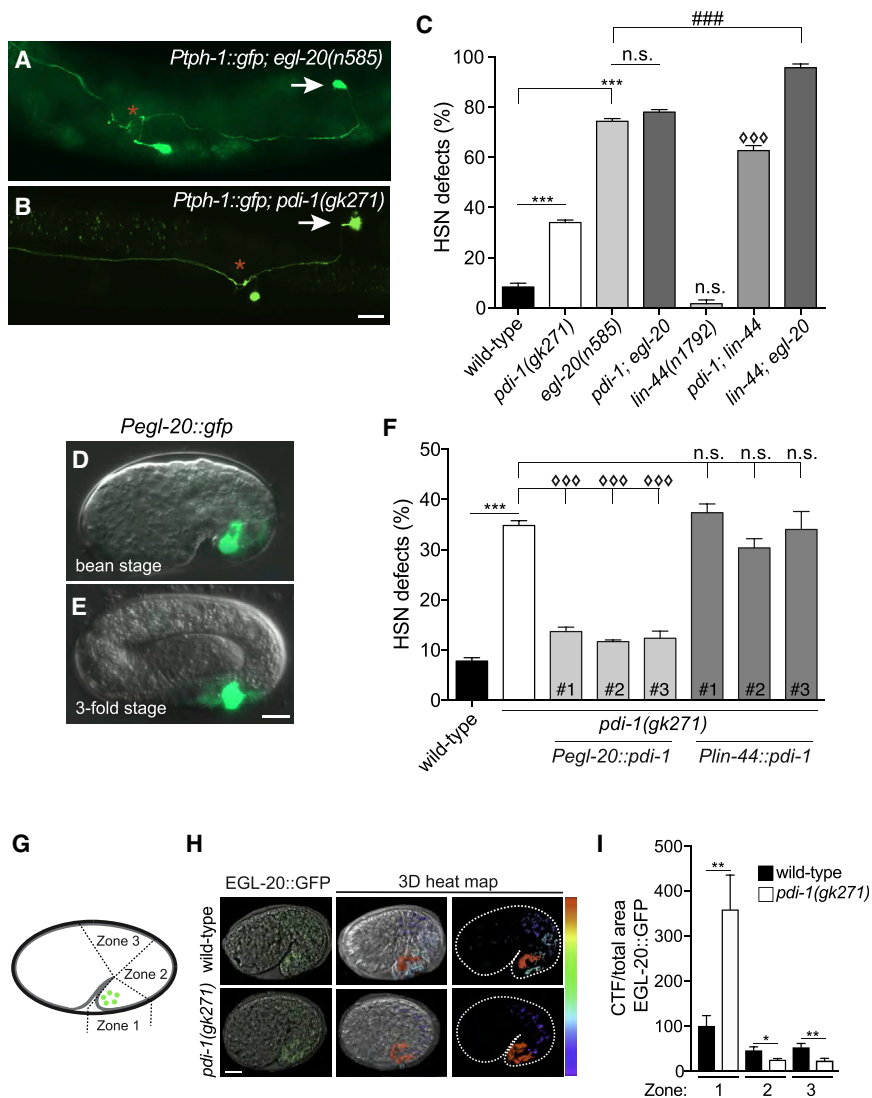


Figure 3. PDI-1 Acts in the EGL-20/Wnt Pathway to Direct HSN Migration

(A and B) HSN anatomy of *egl-20(n585)* (A) and *pdi-1(gk271)* (B) mutant animals (HSN under-migration, white arrows). Vulval position, red asterisk. Ventral view, anterior is to the left. Scale bar: 20 μ m.

(C) Double-mutant analysis of Wnt morphogen mutant strains in combination with *pdi-1(gk271)*. See Table S1 for detailed scoring. $n > 50$; *** $p < 0.001$ for wild-type compared to *pdi-1* and *egl-20* mutants; ◇◇◇ $p < 0.001$ for *pdi-1(gk271)* compared to *pdi-1(gk271); lin-44(n1792)* double mutant; ### $p < 0.001$ for *egl-20(n585); lin-44(n1792)* double mutant; n.s., not significant.

(D and E) Expression of a *Pegl-20::gfp* transcriptional reporter at the comma (D) and 3-fold (E) stages of embryonic development in a subset of posterior cells, as previously shown (Prasad and Clark, 2006; Whangbo and Kenyon, 1999). Anterior is to the left. Scale bar: 10 μ m.

(F) HSN developmental defects of *pdi-1(gk271)* mutant animals are rescued by transgenic expression of *pdi-1* cDNA controlled by the *egl-20* promoter (used in D and E) but not by the *lin-44* promoter, which expresses more posteriorly (Klassen and Shen, 2007). $n > 50$; *** $p = 0.001$ for wild-type compared to *pdi-1(gk271)*; ◇◇◇ $p < 0.001$; n.s., not significant for *pdi-1(gk271)* compared to rescue lines. # refers to independent transgenic lines.

(G–I) EGL-20::GFP expression and secretion analysis.

(G) Schematic of a comma-stage embryo expressing EGL-20::GFP from a group of posterior cells (green circles). EGL-20::GFP levels measured in zones 1–3.

(H) Three-dimensional (3D) reconstruction and heatmap of wild-type and *pdi-1(gk271)* mutant comma-stage embryos expressing EGL-20::GFP. Single slice of a Z stack from confocal microscopy (left) and 3D reconstructed heatmaps of the same embryos (center and right). EGL-20::GFP is represented from high (red) to low (blue).

(I) Corrected total EGL-20::GFP fluorescence of wild-type and *pdi-1(gk271)* animals in each zone of comma-stage embryos. $n = 15$; * $p < 0.05$; ** $p < 0.001$.

proteins contain a C-terminal ER-retention signal (His-Glu-Glu-Leu or HEEL) that helps maintain their functional locale. We deleted this ER retention signal (–HEEL) in PDI-1 and found that this abrogates the ability of PDI-1 to rescue the HSN developmental defects of *pdi-1(–)* animals (Figure 2J). Together, our data show that PDI-1 acts within the ER of hypodermal cells to cell-non-autonomously regulate HSN development.

PDI-1 and EGL-20/Wnt Control HSN Migration in the Same Genetic Pathway

HSN migration defects of *pdi-1(–)* animals are comparable, albeit less severe, to defects of *egl-20/Wnt* loss-of-function animals (Figures 3A–3C; Table S1) (Forrester et al., 2004). We used genetic analysis to determine whether *pdi-1* and *egl-20* act in the

same pathway to direct HSN development (Figure 3C; Table S1). We examined the *egl-20(n585)* missense allele in which a conserved cysteine is substituted to serine (C99S) (Maloo et al., 1999). Mutation of this cysteine in human Wnt3a causes reduced secretion and activity (MacDonald et al., 2014). We show that *egl-20(n585)* causes highly penetrant defects (~75%) in HSN development (Figure 3C), as previously reported (Desai et al., 1988; Forrester et al., 2004; Harris et al., 1996). The *pdi-1(–); egl-20(n585)* compound mutant had no enhanced penetrance or expressivity of HSN defects compared to *egl-20(n585)* (Figure 3C; Table S1), suggesting that these genes act in the same genetic pathway. We considered that the penetrance of HSN defects observed in *egl-20(n585)* animals may have reached a ceiling, and, as such, no enhancement of

phenotype was possible. However, when we introduced a LIN-44/Wnt mutation into the *egl-20(n585)* mutant background, we found that the *egl-20(n585); lin-44(n1972)* compound mutant exhibits increased penetrance of HSN defects when compared to *egl-20(n585)* (Figure 3C; Table S1), as previously shown (Zinovyeva et al., 2008). We also found the *lin-44(n1972)* mutation enhances the *pdi-1(-)* HSN developmental defects (Figure 3C; Table S1). Together, these data show that *pdi-1* acts in the same pathway as *egl-20* and in parallel to *lin-44* to control HSN development.

HSN development is controlled by a complex network of Wnt ligands and Frizzled receptors (Pan et al., 2006; Zinovyeva and Forrester, 2005; Zinovyeva et al., 2008). The Frizzled receptors MIG-1 and CFZ-2 act in a partially overlapping manner to coordinate HSN development, where CFZ-2 function is only revealed when MIG-1 is abrogated (Pan et al., 2006; Zinovyeva et al., 2008). Loss of EGL-20 enhances HSN developmental defects in a *mig-1* mutant (Table S1) but not the *cfz-2* mutant (Zinovyeva and Forrester, 2005), suggesting that EGL-20 can act on both receptors but predominantly on MIG-1. We found that loss of PDI-1 in a *mig-1* mutant causes fully penetrant HSN migration defects (Table S1). In contrast, the penetrance and expressivity of *pdi-1(-); cfz-2(ok1201)* are no different from *pdi-1(-)* (Table S1). Together, these data show that PDI-1 acts through the same signaling pathway as EGL-20 to direct HSN migration.

PDI-1 Functions in EGL-20/Wnt-Producing Cells to Control HSN Migration

PDI-1 and EGL-20 are both expressed in the hypodermis, with EGL-20 expression in a more restricted posterior region (Prasad and Clark, 2006; Whangbo and Kenyon, 1999). If PDI-1 controls EGL-20-directed HSN development, one may expect *pdi-1* to act in *egl-20*-producing hypodermal cells. We used the published 1,900-bp *egl-20* promoter (Harris et al., 1996) to drive *pdi-1* cDNA in *egl-20*-producing cells (Figures 3D and 3E) and found that HSN developmental defects of *pdi-1(-)* animals were fully rescued (Figure 3F). In contrast, expressing *pdi-1* cDNA using the *lin-44* promoter, in an adjacent and non-overlapping subset of cells (Coudreuse et al., 2006; Klassen and Shen, 2007), was unable to rescue the *pdi-1(-)* HSN phenotype (Figure 3F). Thus, PDI-1 acts specifically from EGL-20-producing hypodermal cells to control HSN development.

PDI-1 Controls EGL-20/Wnt Gradient Formation

Formation of an EGL-20 gradient is crucial for correct HSN and Q cell migration in *C. elegans* (Coudreuse et al., 2006; Pan et al., 2006). We hypothesized that loss of PDI-1 function could affect the EGL-20 gradient. Three-dimensional reconstructions of EGL-20::GFP localization in comma-stage embryos reveal that EGL-20 forms an anteroposterior gradient (Figures 3H and S3) (Coudreuse et al., 2006; Pan et al., 2006), and this gradient is perturbed in *pdi-1(-)* animals (Figures 3H and 3I). Loss of PDI-1 elevates EGL-20 localization adjacent to its site of expression with concomitant weaker distal expression (Figures 3G–3I and S3). These results reveal that PDI-1 is involved in a key phase of EGL-20 maturation within EGL-20-expressing cells to enable EGL-20::GFP gradient formation.

A PDI Inhibitor Diminishes Wnt3a Secretion from Human Cells

Most mammalian genomes harbor 19 Wnt and over 20 PDI proteins that exhibit diverse expression domains and biological functions (Ellgaard and Ruddock, 2005; Galligan and Petersen, 2012; Willert and Nusse, 2012). Mammalian Wnt3a secretion is abrogated when individual cysteine residues are substituted to alanine (MacDonald et al., 2014), suggesting that Wnt secretion is influenced by disulfide bond coordination.

To examine the functional conservation of PDIs, we inhibited PDI function in human embryonic kidney cells (HEK293T) with the 16F16 PDI inhibitor (Hoffstrom et al., 2010; Kaplan et al., 2015) and assayed endogenous Wnt3a levels. Using a polyclonal anti-Wnt3a antibody (Abcam; ab199925), which we validated using small interfering RNA (siRNA) knockdown of Wnt3a (Figure S4A), we found that PDI inhibition caused cellular accumulation of Wnt3a (Figures 4A and 4B) (Lim et al., 2010; Vallier et al., 2009). This was not due to increased transcription, as Wnt3a mRNA levels in 16F16-treated cells are unchanged (Figure 4C). To assess Wnt3a secretion, we transfected HEK293T cells with C-terminally V5-tagged Wnt3a (Wnt3a-V5) (Figures 4D and 4E). The 16F16 PDI inhibitor reduced Wnt3a-V5 secretion in a dose-responsive manner (Figures 4D and 4E), with no detectable effect on cell viability (Figure S4B). Conversely, we expressed FLAG-tagged TIG-2 (a bone morphogenetic secreted protein) in HEK293T cells and found that the 16F16 inhibitor had no detectable effect on secretion (Figures S4C–S4F). These data demonstrate that, as in the *C. elegans* embryo, PDIs are important for correct Wnt secretion from human cells and are therefore fundamental regulators of Wnt signaling.

DISCUSSION

Wnt proteins are morphogens that can form long-range concentration gradients to control developmental patterning. Multiple regulatory mechanisms have evolved to control the amplitude, range, and precision of Wnt-directed events. A fundamental question is how Wnt protein folding and maturation is controlled in Wnt-producing cells to enable secretion. Previous studies found that Wnt secretion is controlled by the function of the retromer complex and the Wnt-binding protein Wls (Bänziger et al., 2006; Coudreuse et al., 2006; Yang et al., 2008). Here, we report the discovery of a regulatory mechanism where Wnt secretion is controlled by PDIs.

The complexity of Wnt protein secondary structure is coordinated by intracellular disulfide bonds between conserved and invariantly positioned cysteine residues. We reasoned that specific protein chaperones may control disulfide bond formation, which would be important for Wnt protein secretion. By genetic screening of candidate molecules, we identified that PDI-1 is crucial for EGL-20/Wnt gradient formation in *C. elegans*. To examine the phenotypic consequence of a reduced EGL-20/Wnt gradient in *pdi-1(-)* animals, we analyzed two well-characterized EGL-20/Wnt-dependent neurodevelopmental events. We found that PDI-1 controls the migratory capacity of the HSN and Q cells and performs this function cell-non-autonomously from epidermal cells that co-express EGL-20/Wnt. This

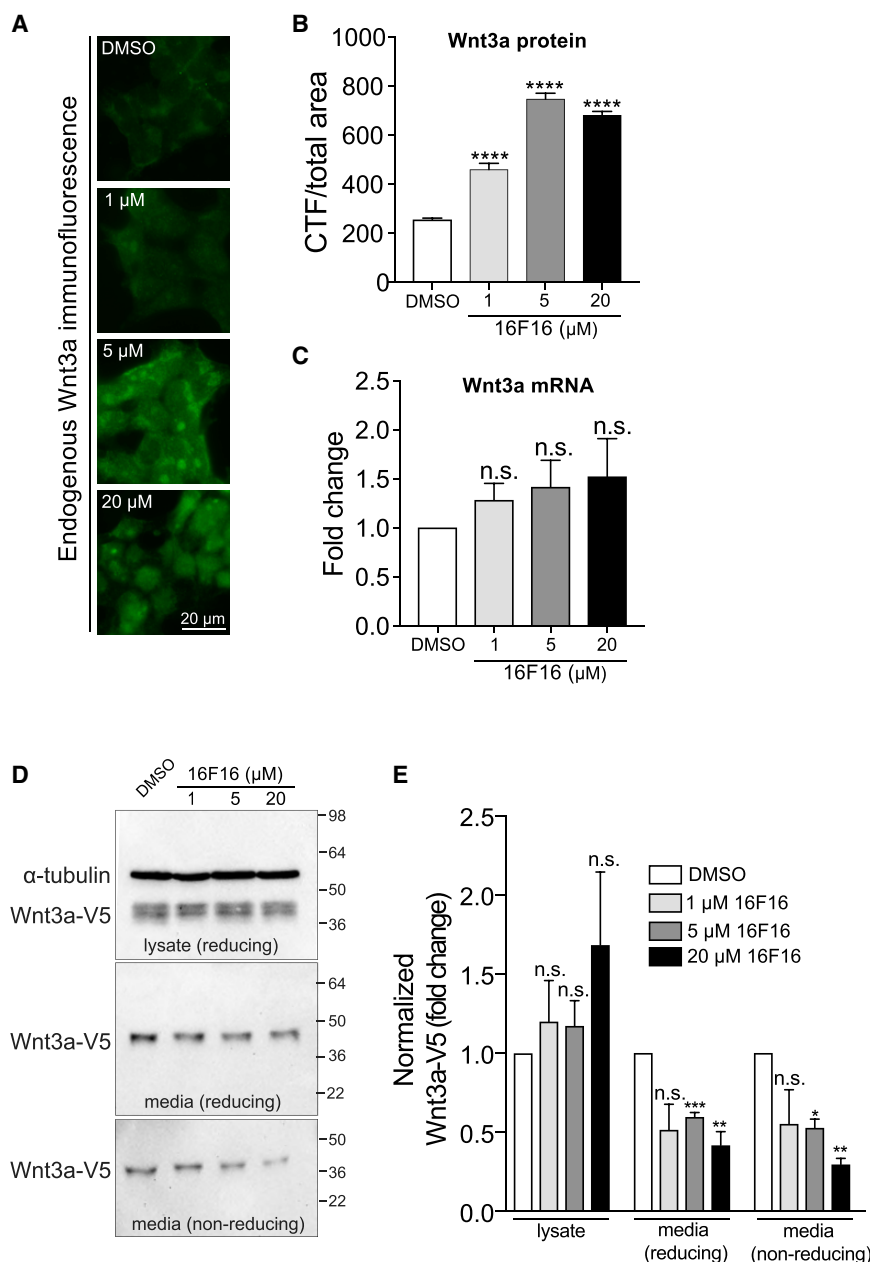


Figure 4. A PDI Inhibitor Reduces Wnt3a Secretion

(A–C) The 16F16 PDI inhibitor increases endogenous Wnt3a protein levels without affecting transcription.

(A) Endogenous Wnt3a immunofluorescence in HEK293T cells incubated with increasing concentrations (0, 1, 5, and 20 μM) of 16F16 in DMSO. Scale bar: 20 μm.

(B) Quantification of endogenous Wnt3a immunofluorescence from (A) shows increased levels of Wnt3a protein. $n > 150$ cells from three independent experiments. **** $p < 0.0001$ compared to DMSO control.

(C) Wnt3a transcription in HEK293T cells is not affected by incubation with 16F16. Measurements were taken in triplicate. n.s., not significant compared to control.

(D and E) Wnt3a-V5 expression in HEK293T cells incubated with increasing concentrations (0, 1, 5, and 20 μM) of 16F16 in DMSO. Western blot analysis was performed using anti-V5 (to detect Wnt3a-V5) and anti-α-tubulin (control). Three western blots from independent samples were performed, a representative example of which is shown in (D), and mean values are depicted in (E). Data are presented as DMSO-control set to 1-fold. * $p < 0.02$; ** $p < 0.07$; *** $p < 0.001$; n.s., not significant compared to DMSO-treated cells.

does not, however, preclude the possibility that PDI-1 controls the secretion and/or functional capacity of other Wnt morphogens in *C. elegans*. The development of Wnt secretion models for the other Wnt morphogens in *C. elegans*—MOM-2, LIN-44, CWN-1, and CWN-2—would enable this interesting question to be examined. Furthermore, other PDI proteins in *C. elegans*—PDI-2, PDI-3, PDI-6, and C14B9.2—may also control secretion of other Wnts in a tissue- and cell-specific manner. PDI expression analysis, phenotypic characterization and Wnt secretion assays in *pdi*(–) backgrounds may identify additional regulatory relationships between PDIs and Wnts. Indeed, differential regulation of Wnt secretion by specific PDIs may reveal a regulatory

logic, perhaps based on protein structural requirements, to facilitate precise regulation of Wnt secretion.

We further showed that pharmacological inhibition of PDIs causes HSN defects that are not enhanced by *pdi-1* loss. This strongly suggests that this PDI inhibitor can abrogate PDI-1 function *in vivo*. We used the same PDI inhibitor in human cells to show that the mechanism we revealed is conserved, where PDI inhibition decreases Wnt3a secretion. A previous study showed the importance of disulfide bonds for human Wnt3A secretion, where specific cysteine-to-alanine substitutions reduced Wnt3a secretion, suggesting that the location of unpaired cysteines has differential effects on Wnt3a secretion

(MacDonald et al., 2014). In addition, wild-type Wnt3a can form erroneous disulfide bonds during maturation, which would need to be reconfigured prior to secretion (MacDonald et al., 2014; Zhang et al., 2012). Our *in vivo* study has revealed that this function is likely performed by disulfide isomerases.

Wnt mutations identified in model organism forward genetic screens and in human disease states also reveal the importance of cysteine residues for Wnt function. Cysteine mutations in the *Drosophila melanogaster* Wnt protein Wingless, C104S and C242Y, cause temperature-sensitive deficits in secretion and null phenotype, respectively (Dierick and Bejsovec, 1998; van den Heuvel et al., 1993). For *C. elegans* EGL-20/Wnt, the C99S

missense mutation behaves as a null allele, whereas the C110Y and C166Y mutations are hypomorphic (Desai et al., 1988; Maloof et al., 1999). In human studies, cysteine mutations in diverse Wnt proteins occur in disease. In Robinow syndrome, characterized by short-limbed dwarfism, a causative mutation in Wnt5a (C182R) and other mutations (C69Y and C83S) have been identified (Person et al., 2010; Robinow et al., 1969; Roifman et al., 2015). In addition, a heterozygous Wnt10b mutation (C256Y) was discovered as a potential obesity-related lesion (Christodoulides et al., 2006). Crucially, these mutations affect Wnt secretion and activity *in vitro* (Christodoulides et al., 2006; MacDonald et al., 2014). Together, these studies support the finding that individual cysteines have differential effects on Wnt function and secretion (MacDonald et al., 2014). The differences may be due to redundancy in the Wnt system, the specific complement of Wnt proteins that are required to drive certain developmental and homeostatic processes, and/or genetic backgrounds. Our genetic data show that loss of PDI-1 in *C. elegans* does not precisely phenocopy the EGL-20/Wnt null (Figure 3). Therefore, a proportion of EGL-20/Wnt protein is likely secreted and functional in *pdi-1(-)* animals. This suggests that additional chaperones are required for folding and secretion of Wnts in laboratory conditions.

In conclusion, Wnt protein structure is coordinated by disulfide bonds that have differential importance for Wnt secretion. During maturation, nascent Wnt proteins can form inappropriate disulfide bonds (MacDonald et al., 2014; Zhang et al., 2012) that need to be resolved prior to release to enable appropriate Wnt signaling. Variations in disulfide bond arrangement may provide additional flexibility for interactions between Wnts and specific receptor molecules. Therefore, the oxidation and rearrangement of disulfide bonds are vital and pervasive steps during Wnt biogenesis—a function we have shown to be mediated by PDIs.

STAR★METHODS

Detailed methods are provided in the online version of this paper and include the following:

- KEY RESOURCES TABLE
- CONTACT FOR REAGENT AND RESOURCE SHARING
- EXPERIMENTAL MODEL AND SUBJECT DETAILS
 - Mutant and transgenic reporter strains
 - Transgenic lines
 - Primary Cell Lines
- METHOD DETAILS
 - Molecular cloning
 - RNAi experiments
 - PDI inhibition in *C. elegans*
 - Fluorescence microscopy of *C. elegans*
 - Nomarski analysis of long-range migrating neurons
 - 3D analysis of EGL-20::GFP distribution in *C. elegans* embryos
 - Endogenous Wnt3a staining of HEK293T cells
 - Wnt3a secretion assay in HEK293T cells
 - Fluorescence-activated cell sorting
 - qPCR assays
- QUANTIFICATION AND STATISTICAL ANALYSIS

SUPPLEMENTAL INFORMATION

Supplemental Information can be found with this article online at <https://doi.org/10.1016/j.celrep.2019.02.072>.

ACKNOWLEDGMENTS

We thank members of the Pocock Laboratory and Brent Neumann for comments on the manuscript. Some strains were provided by the Caenorhabditis Genetics Center (University of Minnesota), which is funded by NIH Office of Research Infrastructure Programs (P40 OD010440). This work was supported by the following grants: Monash University Senior Postdoctoral Fellowship to S.G., NWO-ALW (Open Program Grant 822.02.012) to H.C.K., European Research Council (ERC Starting Grant 260807 to R.P.), Lundbeck Foundation (Project R67-A6094 to R.P.), NHMRC (Project GNT1105374 and Senior Research Fellowship GNT1137645 to R.P.), and veski innovation fellowship (VIF23 to R.P.).

AUTHOR CONTRIBUTIONS

N.T., S.G., O.B., L.R., and R.P. conducted the experiments. S.G., A.H., H.C.K., and R.P. designed the experiments and wrote the paper.

DECLARATION OF INTERESTS

The authors declare no competing interests.

Received: October 20, 2018

Revised: December 10, 2018

Accepted: February 20, 2019

Published: March 19, 2019

REFERENCES

- Bänziger, C., Soldini, D., Schütt, C., Zipperlen, P., Hausmann, G., and Basler, K. (2006). Wntless, a conserved membrane protein dedicated to the secretion of Wnt proteins from signaling cells. *Cell* 125, 509–522.
- Barrott, J.J., Cash, G.M., Smith, A.P., Barrow, J.R., and Murtaugh, L.C. (2011). Deletion of mouse *Porcn* blocks Wnt ligand secretion and reveals an ectodermal etiology of human focal dermal hypoplasia/Goltz syndrome. *Proc. Natl. Acad. Sci. USA* 108, 12752–12757.
- Belenkaya, T.Y., Wu, Y., Tang, X., Zhou, B., Cheng, L., Sharma, Y.V., Yan, D., Selva, E.M., and Lin, X. (2008). The retromer complex influences Wnt secretion by recycling wntless from endosomes to the trans-Golgi network. *Dev. Cell* 14, 120–131.
- Bocchi, R., Egervari, K., Carol-Perdiguer, L., Viale, B., Quairiaux, C., De Roo, M., Boitard, M., Oskouie, S., Salmon, P., and Kiss, J.Z. (2017). Perturbed Wnt signaling leads to neuronal migration delay, altered interhemispheric connections and impaired social behavior. *Nat. Commun.* 8, 1158.
- Braakman, I., and Buleid, N.J. (2011). Protein folding and modification in the mammalian endoplasmic reticulum. *Annu. Rev. Biochem.* 80, 71–99.
- Cadigan, K.M., Fish, M.P., Rulifson, E.J., and Nusse, R. (1998). Wingless repression of *Drosophila* frizzled 2 expression shapes the Wingless morphogen gradient in the wing. *Cell* 93, 767–777.
- Caramelo, J.J., and Parodi, A.J. (2007). How sugars convey information on protein conformation in the endoplasmic reticulum. *Semin. Cell Dev. Biol.* 18, 732–742.
- Christodoulides, C., Scarda, A., Granzotto, M., Milan, G., Dalla Nora, E., Keogh, J., De Pergola, G., Stirling, H., Pannacciulli, N., Sethi, J.K., et al. (2006). WNT10B mutations in human obesity. *Diabetologia* 49, 678–684.
- Clevers, H. (2006). Wnt/beta-catenin signaling in development and disease. *Cell* 127, 469–480.
- Coudreuse, D.Y., Roël, G., Betist, M.C., Destrée, O., and Korswagen, H.C. (2006). Wnt gradient formation requires retromer function in Wnt-producing cells. *Science* 312, 921–924.

- Desai, C., Garriga, G., McIntire, S.L., and Horvitz, H.R. (1988). A genetic pathway for the development of the *Caenorhabditis elegans* HSN motor neurons. *Nature* 336, 638–646.
- Dierick, H.A., and Bejsovec, A. (1998). Functional analysis of Wingless reveals a link between intercellular ligand transport and dorsal-cell-specific signaling. *Development* 125, 4729–4738.
- Ellgaard, L., and Ruddock, L.W. (2005). The human protein disulphide isomerase family: substrate interactions and functional properties. *EMBO Rep.* 6, 28–32.
- Fass, D. (2012). Disulfide bonding in protein biophysics. *Annu. Rev. Biophys.* 41, 63–79.
- Forrester, W.C., Kim, C., and Garriga, G. (2004). The *Caenorhabditis elegans* Ror RTK CAM-1 inhibits EGL-20/Wnt signaling in cell migration. *Genetics* 168, 1951–1962.
- Fraser, A.G., Kamath, R.S., Zipperlen, P., Martinez-Campos, M., Sohrmann, M., and Ahringer, J. (2000). Functional genomic analysis of *C. elegans* chromosome I by systematic RNA interference. *Nature* 408, 325–330.
- Galligan, J.J., and Petersen, D.R. (2012). The human protein disulfide isomerase gene family. *Hum. Genomics* 6, 6.
- Gopal, S., Boag, P., and Pocock, R. (2017). Automated three-dimensional reconstruction of the *Caenorhabditis elegans* germline. *Dev. Biol.* 432, 222–228.
- Grzeschik, K.H., Bornholdt, D., Oeffner, F., König, A., del Carmen Boente, M., Enders, H., Fritz, B., Hertl, M., Grasshoff, U., Höfling, K., et al. (2007). Deficiency of PORCN, a regulator of Wnt signaling, is associated with focal dermal hypoplasia. *Nat. Genet.* 39, 833–835.
- Harris, J., Honigberg, L., Robinson, N., and Kenyon, C. (1996). Neuronal cell migration in *C. elegans*: regulation of Hox gene expression and cell position. *Development* 122, 3117–3131.
- Hilliard, M.A., and Bargmann, C.I. (2006). Wnt signals and frizzled activity orient anterior-posterior axon outgrowth in *C. elegans*. *Dev. Cell* 10, 379–390.
- Hoffstrom, B.G., Kaplan, A., Letso, R., Schmid, R.S., Turmel, G.J., Lo, D.C., and Stockwell, B.R. (2010). Inhibitors of protein disulfide isomerase suppress apoptosis induced by misfolded proteins. *Nat. Chem. Biol.* 6, 900–906.
- Janda, C.Y., Waghay, D., Levin, A.M., Thomas, C., and Garcia, K.C. (2012). Structural basis of Wnt recognition by Frizzled. *Science* 337, 59–64.
- Kadowaki, T., Wilder, E., Klingensmith, J., Zachary, K., and Perrimon, N. (1996). The segment polarity gene porcupine encodes a putative multitransmembrane protein involved in Wingless processing. *Genes Dev.* 10, 3116–3128.
- Kaplan, A., Gaschler, M.M., Dunn, D.E., Colligan, R., Brown, L.M., Palmer, A.G., 3rd, Lo, D.C., and Stockwell, B.R. (2015). Small molecule-induced oxidation of protein disulfide isomerase is neuroprotective. *Proc. Natl. Acad. Sci. USA* 112, E2245–E2252.
- Kennedy, L.M., Pham, S.C., and Grishok, A. (2013). Nonautonomous regulation of neuronal migration by insulin signaling, DAF-16/FOXO, and PAK-1. *Cell Rep.* 4, 996–1009.
- Klassen, M.P., and Shen, K. (2007). Wnt signaling positions neuromuscular connectivity by inhibiting synapse formation in *C. elegans*. *Cell* 130, 704–716.
- Lim, B.K., Cho, S.J., Sumbre, G., and Poo, M.M. (2010). Region-specific contribution of ephrin-B and Wnt signaling to receptive field plasticity in developing optic tectum. *Neuron* 65, 899–911.
- MacDonald, B.T., Hien, A., Zhang, X., Iranloye, O., Virshup, D.M., Waterman, M.L., and He, X. (2014). Disulfide bond requirements for active Wnt ligands. *J. Biol. Chem.* 289, 18122–18136.
- Mallof, J.N., Whangbo, J., Harris, J.M., Jongeward, G.D., and Kenyon, C. (1999). A Wnt signaling pathway controls hox gene expression and neuroblast migration in *C. elegans*. *Development* 126, 37–49.
- Mello, C.C., Kramer, J.M., Stinchcomb, D., and Ambros, V. (1991). Efficient gene transfer in *C. elegans*: extrachromosomal maintenance and integration of transforming sequences. *EMBO J.* 10, 3959–3970.
- Miller, J.R. (2002). The Wnts. *Genome Biol.* 3, REVIEWS3001.
- Pan, C.L., Howell, J.E., Clark, S.G., Hilliard, M., Cordes, S., Bargmann, C.I., and Garriga, G. (2006). Multiple Wnts and frizzled receptors regulate anteriorly directed cell and growth cone migrations in *Caenorhabditis elegans*. *Dev. Cell* 10, 367–377.
- Pedersen, M.E., Snieckute, G., Kagias, K., Nehammer, C., Mulhaupt, H.A., Couchman, J.R., and Pocock, R. (2013). An epidermal microRNA regulates neuronal migration through control of the cellular glycosylation state. *Science* 341, 1404–1408.
- Person, A.D., Beiraghi, S., Sieben, C.M., Hermanson, S., Neumann, A.N., Robu, M.E., Schleiffarth, J.R., Billington, C.J., Jr., van Bokhoven, H., Hoogboom, J.M., et al. (2010). WNT5A mutations in patients with autosomal dominant Robinow syndrome. *Dev. Dyn.* 239, 327–337.
- Port, F., Kuster, M., Herr, P., Furger, E., Bänziger, C., Hausmann, G., and Basler, K. (2008). Wingless secretion promotes and requires retromer-dependent cycling of Wntless. *Nat. Cell Biol.* 10, 178–185.
- Prasad, B.C., and Clark, S.G. (2006). Wnt signaling establishes anteroposterior neuronal polarity and requires retromer in *C. elegans*. *Development* 133, 1757–1766.
- Robinow, M., Silverman, F.N., and Smith, H.D. (1969). A newly recognized dwarfing syndrome. *Am. J. Dis. Child.* 117, 645–651.
- Roifman, M., Marcelis, C.L., Paton, T., Marshall, C., Silver, R., Lohr, J.L., Yntema, H.G., Venselaar, H., Kayserili, H., van Bon, B., et al.; FORGE Canada Consortium (2015). De novo WNT5A-associated autosomal dominant Robinow syndrome suggests specificity of genotype and phenotype. *Clin. Genet.* 87, 34–41.
- Takada, R., Satomi, Y., Kurata, T., Ueno, N., Norioka, S., Kondoh, H., Takao, T., and Takada, S. (2006). Monounsaturated fatty acid modification of Wnt protein: its role in Wnt secretion. *Dev. Cell* 11, 791–801.
- Vallier, L., Touboul, T., Chng, Z., Brimpari, M., Hannan, N., Millan, E., Smithers, L.E., Trotter, M., Rugg-Gunn, P., Weber, A., and Pedersen, R.A. (2009). Early cell fate decisions of human embryonic stem cells and mouse epiblast stem cells are controlled by the same signalling pathways. *PLoS ONE* 4, e6082.
- van den Heuvel, M., Harryman-Samos, C., Klingensmith, J., Perrimon, N., and Nusse, R. (1993). Mutations in the segment polarity genes wingless and porcupine impair secretion of the wingless protein. *EMBO J.* 12, 5293–5302.
- Whangbo, J., and Kenyon, C. (1999). A Wnt signaling system that specifies two patterns of cell migration in *C. elegans*. *Mol. Cell* 4, 851–858.
- Wilkinson, B., and Gilbert, H.F. (2004). Protein disulfide isomerase. *Biochim. Biophys. Acta* 1699, 35–44.
- Willert, K., and Nusse, R. (2012). Wnt proteins. *Cold Spring Harb. Perspect. Biol.* 4, a007864.
- Willert, K., Brown, J.D., Danenberg, E., Duncan, A.W., Weissman, I.L., Reya, T., Yates, J.R., 3rd, and Nusse, R. (2003). Wnt proteins are lipid-modified and can act as stem cell growth factors. *Nature* 423, 448–452.
- Yang, P.T., Lorenowicz, M.J., Silhankova, M., Coudreuse, D.Y., Betist, M.C., and Korswagen, H.C. (2008). Wnt signaling requires retromer-dependent recycling of MIG-14/Wntless in Wnt-producing cells. *Dev. Cell* 14, 140–147.
- Yoshikawa, S., McKinnon, R.D., Kokel, M., and Thomas, J.B. (2003). Wnt-mediated axon guidance via the *Drosophila* Derailed receptor. *Nature* 422, 583–588.
- Zhang, X., Abreu, J.G., Yokota, C., MacDonald, B.T., Singh, S., Coburn, K.L., Cheong, S.M., Zhang, M.M., Ye, Q.Z., Hang, H.C., et al. (2012). Tiki1 is required for head formation via Wnt cleavage-oxidation and inactivation. *Cell* 149, 1565–1577.
- Zinovyeva, A.Y., and Forrester, W.C. (2005). The *C. elegans* Frizzled CFZ-2 is required for cell migration and interacts with multiple Wnt signaling pathways. *Dev. Biol.* 285, 447–461.
- Zinovyeva, A.Y., Yamamoto, Y., Sawa, H., and Forrester, W.C. (2008). Complex network of Wnt signaling regulates neuronal migrations during *Caenorhabditis elegans* development. *Genetics* 179, 1357–1371.

STAR★METHODS

KEY RESOURCES TABLE

REAGENT or RESOURCE	SOURCE	IDENTIFIER
Antibodies		
Mouse monoclonal anti-V5 (clone SV5-pk1)	BioRad	MCA1630
Rabbit polyclonal anti-Wnt3a	Abcam	ab199925
Mouse monoclonal anti- α -tubulin (clone 12G10)	Developmental Studies Hybridoma Bank	AB1157911
Mouse monoclonal anti-FLAG	Sigma	F1804
Bacterial and Virus Strains		
Bacteria <i>Escherichia coli</i> HT115	Caenorhabditis Genetics Center (CGC)	N/A
Genotype: <i>E. coli</i> [F ⁻ , mcrA, mcrB, IN(rrnD-rrnE)1, rnc14::Tn10(DE3 lysogen: lavUV5 promoter -T7 polymerase)].		
Bacteria <i>Escherichia coli</i> OP50 (uracil auxotroph)	Caenorhabditis Genetics Center (Cgc)	N/A
Chemicals, Peptides, and Recombinant Proteins		
Tetracycline	Sigma	87128
16F16	Sigma	SML0021
DMSO	Sigma	D2650
Sodium azide	Sigma	S8032-25G
DMEM	Life Technologies	11960044
L-glutamine	Life Technologies	25030-081
Formaldehyde (37%)	Sigma	F8775-25ML
Lipofectamine 2000	Thermo Fisher	11668019
2.5x LDS sample buffer	Thermo Scientific	B0007
Reducing agent	Thermo Scientific	NP0009
propidium iodide	Thermo Fisher	P3566
UltraPure Agarose	Thermo Scientific	16500-500
Ampicillin sodium salt	Sigma	A9518-5G
Critical Commercial Assays		
ImProm-II Reverse Transcription System	Promega	A3800
The LightCycler® 480 SYBR Green I Master	Roche	4707516001
Fast SYBR Green Master Mix	Thermo Scientific	4385610
RNAeasy mini kit	QIAGEN	74104
Experimental Models: Cell Lines		
HEK293T- immortalized embryonic kidney cell, female (transformed with SV40 Large T)	ATCC	Cat# CRL-1573; RRID:CVCL_0045
Experimental Models: Organisms/Strains		
<i>C. elegans</i> : Strain CF1045: <i>muls49[Pegl-20::egl-20::GFP]</i>	This study	WormBase ID: CF1045
<i>C. elegans</i> : Strain RJP133: <i>zdis13[Ptph-1::gfp]</i>	This study	RJP133
<i>C. elegans</i> : Strain RJP849: <i>pdi-1(gk271); zdis13[Ptph-1::gfp]</i>	This study	RJP849
<i>C. elegans</i> : Strain RJP1696: <i>egl-20(n585) zdis13[Ptph-1::gfp]</i>	This study	RJP849
<i>C. elegans</i> : Strain RJP1698: <i>lin-44(n1792); zdis13[Ptph-1::gfp]</i>	This study	RJP1696
<i>C. elegans</i> : Strain RJP1700: <i>cfz-2(ok1201); zdis13[Ptph-1::gfp]</i>	This study	RJP1700
<i>C. elegans</i> : Strain RJP1700: <i>pdi-1(gk271); egl-20(n585) zdis13 [Ptph-1::gfp]</i>	This study	RJP1700
<i>C. elegans</i> : Strain RJP1700: <i>lin-44(n1792); pdi-1(gk271); zdis13 [Ptph-1::gfp]</i>	This study	RJP1700

(Continued on next page)

Continued

REAGENT or RESOURCE	SOURCE	IDENTIFIER
<i>C. elegans</i> : Strain RJP1703: <i>mig-1(e1787); pdi-1(gk271); zlds13[Ptph-1::gfp]</i>	This study	RJP1703
<i>C. elegans</i> : Strain RJP1704: <i>cfz-2(ok1201); pdi-1(gk271); zlds13[Ptph-1::gfp]</i>	This study	RJP1704
<i>C. elegans</i> : Strain RJP3989: <i>mig-1(e1787); egl-20(n585) zlds13[Ptph-1::gfp]</i>	This study	RJP3989
<i>C. elegans</i> : Strain RJP1688: <i>rpEx715[Ppdi-1::gfp]</i>	This study	RJP1688
<i>C. elegans</i> : Strain RJP1725: <i>rpEx733[Pegl-20::gfp]</i>	This study	RJP1725
<i>C. elegans</i> : Strain RJP845: <i>pdi-1(gk271); zlds13[Ptph-1::gfp]; rpEx429[Ppdi-1:: pdi-1 cDNA]</i>	This study	RJP845
<i>C. elegans</i> : Strain RJP1691: <i>pdi-1(gk271); zlds13[Ptph-1::gfp]; rpEx718[Ppdi-1:: pdi-1 cDNA]</i>	This study	RJP1691
<i>C. elegans</i> : Strain RJP1692: <i>pdi-1(gk271); zlds13[Ptph-1::gfp]; rpEx719[Ppdi-1:: pdi-1 cDNA]</i>	This study	RJP1692
<i>C. elegans</i> : Strain RJP842: <i>pdi-1(gk271); zlds13[Ptph-1::gfp]; rpEx426[Pdpy-7:: pdi-1 cDNA]</i>	This study	RJP842
<i>C. elegans</i> : Strain RJP843: <i>pdi-1(gk271); zlds13[Ptph-1::gfp]; rpEx427[Pdpy-7:: pdi-1 cDNA]</i>	This study	RJP843
<i>C. elegans</i> : Strain RJP844: <i>pdi-1(gk271); zlds13[Ptph-1::gfp]; rpEx428[Pdpy-7:: pdi-1 cDNA]</i>	This study	RJP844
<i>C. elegans</i> : Strain RJP1251: <i>pdi-1(gk271); zlds13[Ptph-1::gfp]; rpEx583[Pdpy-7:: pdi-1 cDNA -HEEL]</i>	This study	RJP1251
<i>C. elegans</i> : Strain RJP1252: <i>pdi-1(gk271); zlds13[Ptph-1::gfp]; rpEx584[Pdpy-7:: pdi-1 cDNA -HEEL]</i>	This study	RJP1252
<i>C. elegans</i> : Strain RJP1253: <i>pdi-1(gk271); zlds13[Ptph-1::gfp]; rpEx585[Pdpy-7:: pdi-1 cDNA -HEEL]</i>	This study	RJP1253
<i>C. elegans</i> : Strain RJP1693: <i>pdi-1(gk271); zlds13[Ptph-1::gfp]; rpEx720[Pegl-20:: pdi-1 cDNA]</i>	This study	RJP1693
<i>C. elegans</i> : Strain RJP1694: <i>pdi-1(gk271); zlds13[Ptph-1::gfp]; rpEx721[Pegl-20:: pdi-1 cDNA]</i>	This study	RJP1694
<i>C. elegans</i> : Strain RJP1695: <i>pdi-1(gk271); zlds13[Ptph-1::gfp]; rpEx722[Pegl-20:: pdi-1 cDNA]</i>	This study	RJP1695
<i>C. elegans</i> : Strain RJP3985: <i>pdi-1(gk271); zlds13[Ptph-1::gfp]; rpEx1717[Plin-44:: pdi-1 cDNA]</i>	This study	RJP3985
<i>C. elegans</i> : Strain RJP3986: <i>pdi-1(gk271); zlds13[Ptph-1::gfp]; rpEx1718[Plin-44:: pdi-1 cDNA]</i>	This study	RJP3986
<i>C. elegans</i> : Strain RJP3987: <i>pdi-1(gk271); zlds13[Ptph-1::gfp]; rpEx1719[Plin-44:: pdi-1 cDNA]</i>	This study	RJP3987
Oligonucleotides		
SMARTpool: siGENOME Wnt3A siRNA	Dharmacon	M-008538-00-0005
Recombinant DNA		
Plasmid: pPD49.26- <i>Ppdi-1::pdi-1</i>	This study	N/A
Plasmid: <i>Pdpy-7::pdi-1</i> cDNA	This study	N/A
Plasmid: pPD49.26- <i>Pdpy-7::pdi-1</i> cDNA -HEEL rescue construct	This study	N/A
Plasmid: pPD49.26- <i>Pegl-20::pdi-1</i> cDNA	This study	N/A
Plasmid: pPD49.26- <i>Plin-44::pdi-1</i> cDNA	This study	N/A
Plasmid: pPD95.75- <i>Pegl-20::gfp</i> reporter	This study	N/A
Plasmid: pcDNA3.1(zeo)::pdi-1 cDNA::HIS tag	This study	N/A
Plasmid: pcDNA3.1(zeo)::egl-20 cDNA::FLAG tag	This study	N/A
Plasmid: pcDNA3.1(zeo)::tig-2 cDNA::FLAG tag	This study	N/A

(Continued on next page)

Continued

REAGENT or RESOURCE	SOURCE	IDENTIFIER
Plasmid: pPD49.26- <i>pmyo-2::mCherry</i>	This study	N/A
Plasmid: Wnt3A-V5	Addgene MacDonald et al. J Biol Chem. 2014	43810
Software and Algorithms		
ImageJ 1.47n	National Institute of Health, USA	N/A
Imaris 9.1.2	Bitplane	N/A

CONTACT FOR REAGENT AND RESOURCE SHARING

Further information and requests for resources and reagents should be directed to and will be fulfilled by the Lead Contact, Roger Pocock (roger.pocock@monash.edu).

EXPERIMENTAL MODEL AND SUBJECT DETAILS

Mutant and transgenic reporter strains

Strains were grown using standard growth conditions on NGM agar at 20°C on *Escherichia coli* OP50, unless otherwise stated. Neuroanatomical reporter strains used - *mgIs70 ls[Ptph-1::gfp]; zdlIs13: ls[Ptph-1::gfp]*. Detailed strain information is detailed in Table S2.

Transgenic lines

Rescue constructs were injected into the *pdi-1(gk271)* mutant background at 5-15 ng/μl with *Pmyo-2::mCherry* (5 ng/μl) as injection marker. Expression constructs were injected into N2 (wild-type) background at 50 ng/μl with *Pmyo-2::mCherry* (5 ng/μl) as injection marker. Microinjections were performed using standard methods (Mello et al., 1991). Briefly, young adult worms were picked to an agarose pad covered with oil on a glass slide. The immobilized worms were injected using FemtoJet 4x injector (Eppendorf) controlled by InjectMan 4 (Eppendorf).

Primary Cell Lines

Human Embryonic Kidney cells (female) transformed with SV40 large T were used for transfecting with *Wnt3a* or *tig-2* plasmids and to study endogenous *Wnt3a* expression.

METHOD DETAILS

Molecular cloning

Ppdi-1::pdi-1 cDNA rescue construct

The *Ppdi-1::pdi-1* cDNA rescue construct was generated by cloning the 841 bp *pdi-1* promoter with *SphI-SmaI* into the pPD49.26 vector and then the *pdi-1* cDNA was cloned into this vector using *NheI-SacI*.

Pdpy-7::pdi-1 cDNA rescue construct

The *Pdpy-7::pdi-1* cDNA rescue construct was generated by cloning *pdi-1* cDNA with *NheI-SacI* into a *dpy-7* expression vector.

Pdpy-7::pdi-1 cDNA - HEEL rescue construct

The *Pdpy-7::pdi-1* cDNA -HEEL rescue construct was generated using site-directed mutagenesis to remove the 12 nucleotides that encode HEEL at the C terminus of the PDI-1 protein.

Pegl-20::pdi-1 cDNA rescue construct

The *Pegl-20::pdi-1* cDNA rescue construct was generated by cloning the 1910 bp *egl-20* promoter with *SphI-SmaI* into the pPD49.26 vector containing the *pdi-1* cDNA.

Plin-44::pdi-1 cDNA rescue construct

The *Plin-44::pdi-1* cDNA rescue construct was generated by cloning the 1150 bp *lin-44* promoter with *SphI-SmaI* into the pPD49.26 vector containing the *pdi-1* cDNA.

Pegl-20::gfp reporter construct

The *Pegl-20::gfp* reporter construct was generated by cloning the 1910 bp *egl-20* promoter with *SphI-SmaI* into the promoter-less *gfp* pPD95.75 expression vector.

pcDNA3.1(zeo)::tig-2 cDNA::FLAG tag

The *tig-2*cDNA::FLAG mammalian expression construct was generated by cloning the 1098 bp *tig-2* cDNA with *NheI-HindIII* into the pcDNA3.1(zeo) expression vector.

RNAi experiments

RNAi feeding experiments were conducted following the Ahringer lab protocol (Fraser et al., 2000). L4440 vectors (with or without specific dsRNA) were amplified in *E. coli* HT115 and selected with ampicillin and tetracycline. 100 μ L of bacteria containing L4440 vectors (with or without specific dsRNA) were inoculated on RNAi plates and dried for 24 hr. 3–5 L4 hermaphrodites were moved onto each RNAi bacteria seeded plate and progeny were scored after 4 days as young adults. For each knockdown strain, experiments were conducted on three independent days.

PDI inhibition in *C. elegans*

A 4 μ M solution of the 16F16 small-molecule PDI inhibitor (Sigma - SML0021) was made using M9 buffer (0.1% DMSO final concentration). Synchronized L4 hermaphrodites were incubated in 10 mL of 16F16 (4 μ M) in M9 supplemented with 300 μ L of concentrated OP50 *E. coli*. For the control experiment, worms were incubated in 10 mL of M9 (0.1% DMSO) plus 300 μ L of concentrated OP50 *E. coli*. Worms were shaken at 20°C for 48 hours, after which they were centrifuged at 2500 rpm for 1 minute and then transferred to standard NGM plates seeded with OP50 *E. coli*. HSN anatomy was scored the following day.

Fluorescence microscopy of *C. elegans*

Animals were anesthetized with 20 mM NaN₃ on 5% agarose pads, and images were obtained with an Axio Imager M2 fluorescence microscope and Zen software (Zeiss).

Nomarski analysis of long-range migrating neurons

The final position of Q cell descendants (QR.pax and QL.pax) and HSNs was determined using Nomarski optics in late L1 larvae. The position of QR.pax, QL.pax and HSNs was determined with respect to the seam cell daughters V1.a to V6.p.

3D analysis of EGL-20::GFP distribution in *C. elegans* embryos

Comma stage wild-type and *pdi-1(gk271)* embryos expressing EGL-20::GFP were imaged with a Leica SP5 Confocal microscope using a HC PL APO 63x/1.4 oil objective. Image slices of 0.22 μ m were processed using Adobe Illustrator CC 2018. 3D models of embryos were generated using Imaris 9.1.2 3D interactive microscopy analysis software from Bitplane (Gopal et al., 2017). EGL-20::GFP intensity was calculated after projecting the 3D slices to a 2D plane using FIJI image analysis software (Figure S3). To score EGL-20::GFP distribution, embryos were divided into three zones. Zone 1 encompasses the immediate vicinity of EGL-20::GFP-producing cells, with Zones 2 and 3 covering more distal regions. Background values were obtained from an area of the embryo without detectable EGL-20::GFP. 15 embryos were analyzed from three independent experiments.

Endogenous Wnt3a staining of HEK293T cells

HEK293T cells were cultured overnight in 12-well tissue culture plates in DMEM containing 10% serum and 2.5 mM L-glutamine before treating with 250 μ L media containing 16F16 or DMSO for 16 h. Cells were fixed using 4% paraformaldehyde and stained with anti-Wnt3a antibody and imaged using Zeiss PLAN-APOCHROMAT 40x/1.4 objective. Wnt3a immunofluorescence was quantified using FIJI with the following formula: Corrected total fluorescence (CTF) = Integrated Density – (Area of selected cell x Mean fluorescence of background readings). Wnt3a level from at least 150 cells from three independent experiments was measured. The specificity of the anti-Wnt3a antibody was tested by RNAi followed by immunostaining. Briefly, a monolayer of HEK293T cells in a 12 well plate was transfected with 50 pmol of siRNA (SMARTpool: siGENOME Wnt3a; Dharmacon; M-008538-00-0005) against Wnt3a using Lipofectamine 2000 (Thermo Fisher, 11668019), according to manufacturer instructions. First 50 pmol of siRNA and Lipofectamine 2000 was separately diluted in 100 μ L Opti-MEM and incubated for 5 min at room temperature. The two solutions were combined and incubated for 25 min at room temperature. After incubation, the mixture was added to the monolayer of cells. Transfected cells were incubated at 37°C for 36 hr before staining for Wnt3A protein.

Wnt3a secretion assay in HEK293T cells

HEK293T cells were cultured at 37°C in 12-well tissue culture plates in DMEM containing 10% serum and 2.5 mM L-glutamine. Cells were transfected with Wnt3a-V5 (Addgene, 43810) or TIG-2-FLAG using Lipofectamine 2000 (Thermo Fisher, 11668019), according to manufacturer instructions. Briefly, 1.5 μ g of DNA and Lipofectamine 2000 was diluted in 100 μ L Opti-MEM and incubated for 5 min at room temperature. The two solutions were combined and incubated for 25 min at room temperature. The combined solution was added directly to the cells. After 24 h, the media was replaced with 250 μ L of serum-free DMEM containing the 16F16 PDI inhibitor (Sigma, SML0021) or DMSO. Cells were incubated at 37°C for 16 h before cells and media were collected. The cells were lysed with 50 μ L of 2.5x LDS sample buffer (Thermo Scientific, B0007) containing reducing agent (Thermo Scientific, NP0009). 20 μ L of 2.5x LDS sample buffer, with or without reducing agent, was added to the collected media. Samples were run on an SDS-PAGE gel before blotting to a PVDF membrane. Membranes were probed with antibodies against FLAG (Sigma, F1804) and V5-tag (Bio-Rad, MCA1396GA), and α -tubulin (Developmental Studies Hybridoma Bank, 12G10 anti- α -tubulin) before applying HRP conjugated secondary antibodies (Thermo Scientific). Blots were developed using BioRad ChemiDoc XRS+. Wnt3a band intensity was quantified using FIJI image analysis software. The background was subtracted from each measurement and values were normalized first against α -tubulin and then against DMSO-treated samples.

Fluorescence-activated cell sorting

Cell death after 16F16 treatment of HEK293T was analyzed by propidium iodide (PI) staining followed by FACS. Cells were cultured in 10 cm dishes and were treated with 16F16 (1, 5 or 20 μ M) or DMSO for 16 h, after which cells were harvested using dissociation buffer and stained with PI at a ratio of 1:50. The percentage of PI-stained cells was determined using FACS. For each concentration, at least 100,000 cells were analyzed. The samples were gated in such a way to avoid cell aggregates. PI was maintained in the solution during the analysis.

qPCR assays

Total RNA was isolated using the RNeasy minikit (QIAGEN 74104), according to manufacturer instructions. 500 ng of RNA was reverse-transcribed to cDNA using 0.5 μ g/ μ l oligodT primers and the ImProm-II Reverse Transcription System (A3800) followed. cDNA was diluted to 1:5 in RNAase-free water. Quantitative PCR was performed using Light Cycler 480 (Roche) and SYBR green (Thermo Scientific 4385610). the human Ets2 reference gene was used as a control.

QUANTIFICATION AND STATISTICAL ANALYSIS

All experiments were performed in three independent replicates. The exact numbers of animals/cells analyzed for specific experiments are reported in the figure legends. Statistical analysis was performed in GraphPad Prism 7 using one-way analysis of variance (ANOVA) for comparison followed by Dunnett's Multiple Comparison Test or Tukey's Multiple Comparison Test, where applicable (Figures 1B, 1E, 2J, 3C, 3F, 4B, 4C, and S1). Values are expressed as mean \pm s.d. Differences with a p value < 0.05 considered significant. Statistical analysis of QR/QL descendants was performed using Fisher's exact test (Figure 1D). A Monte Carlo approximation, iterated 10.000 times using SPS Statistics version 22, was used to evaluate significance. Statistical analysis of EGL-20::GFP levels and Wnt-3a secretion was performed using Welch's t test (Figures 3I, 4E, and S4).